

Exact Bayesian inference for level-set Cox processes

Flavio B. Gonçalves and Barbara C. C. Dias

Universidade Federal de Minas Gerais, Brazil

October 17, 2021

Abstract

This paper proposes a class of multidimensional Cox processes in which the intensity function is piecewise constant and develops a methodology to perform Bayesian inference without the need to resort to discretisation-based approximations. Poisson processes with piecewise constant intensity functions are believed to be suitable to model a variety of point process phenomena and, given its simpler structure, are expected to provide more precise inference when compared to processes with non-parametric intensity functions that vary continuously across the space. The piecewise constant property is determined by a level-set function of a latent Gaussian process so that the regions in which the intensity function is constant are defined in a flexible manner. Despite the intractability of the likelihood function and the infinite dimensionality of the parameter space, inference is performed exactly, in the sense that no space discretisation approximation is used and Monte Carlo error is the only source of inaccuracy. That is achieved by using retrospective sampling techniques and devising a pseudo-marginal infinite-dimensional MCMC algorithm that converges to the exact target posterior distribution. An extension to consider spatiotemporal models is also proposed. The efficiency of the proposed methodology is investigated in simulated examples and its applicability is illustrated in the analysis of some real point process datasets.

Keywords: Gaussian process, Pseudo-marginal MCMC, Poisson estimator, retrospective sampling.

1 Introduction

Point pattern statistical models aim at modelling the occurrence of a given event of interest in some region. This is often a compact region in \mathbb{R}^2 such that each data point is interpreted as the location of occurrence of a given event of interest. The most widely used point process model is the Poisson process (PP), in which the number of events in any region has Poisson distribution and is independent for disjoint regions. The Poisson process dynamics is mainly determined by its intensity function (IF) which, roughly speaking, determines the instant rate of occurrence of the event of interest across the region being considered. If the IF is assumed to vary stochastically, the resulting process is called a Cox process. Several classes of Cox process models have already been proposed in the literature,

including non-parametric models in which the IF varies continuously as function of a latent Gaussian process (Møller et al., 1998; Gonçalves and Gamerman, 2018). For several of the real examples considered to fit those models, inference results suggest that a piecewise constant IF ought to be suitable to accommodate the variability of the observed process. Figure 1 shows three examples of estimated intensity functions regarding: white oaks in Lansing Woods, USA, particles in a bronze filter section profile and fires in a region of New Brunswick, Canada. All the datasets are available in the R package `spatstat` (Baddeley et al., 2015) and are revisited in the analyses presented in Section 5. The IF estimates are obtained via kernel smoothing using the R package `splanx` (Rowlingson et al., 2012). Results suggest that a piecewise constant IF assuming up to five different values should be suitable to fit those datasets. This is based on the variance behavior of the Poisson process given its IF which, in turn, is based on the variance of the Poisson distribution.

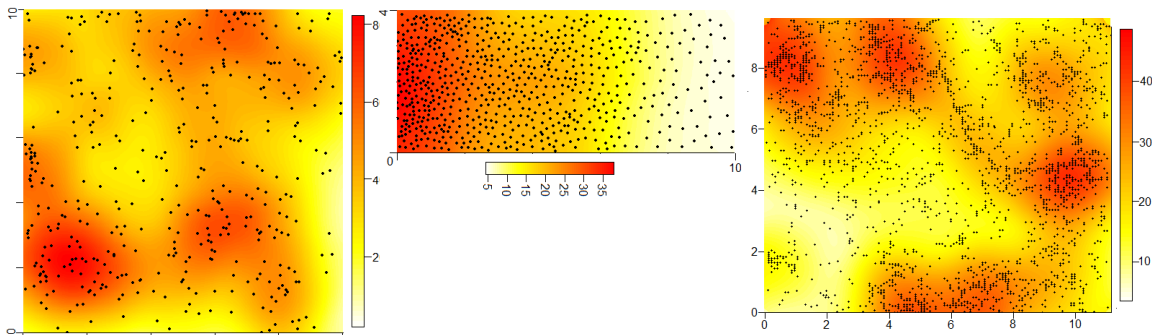


Figure 1: Examples of continuously varying estimated intensity function of Poisson processes. From left to right: white oaks in Lansing Wood, particles in a bronze filter and fires in New Brunswick.

The first aim of this paper is to propose a class of Cox process models with piecewise constant intensity function that is able to define the subregions in which the IF is constant in a flexible way. The motivation is to have models that are suitable to explain and predict the variability of point process phenomena, yet providing more precise estimates than methodologies with continuously varying IF's. The proposed model is based on the level-set structure proposed in Dunlop et al. (2016) to define a piecewise constant function in a given space by means of the levels of a latent Gaussian process (GP). This means that each subregion in which the intensity function is constant is defined by the region in which a latent Gaussian processes assumes values in a given interval. This construction is considerably flexible to define space partitions, allowing for various shapes and sizes of the subregions, including disjoint regions with the same IF. We call the resulting process a *level-set Cox process*.

The second aim of this paper is to devise an exact methodology to perform Bayesian inference for level-set Cox process models. The term exact stems from the fact that no discrete space approximation is assumed and Monte Carlo error is the only source of inaccuracy. This is not a trivial task due to: i) the intractability of the likelihood function of the proposed model (to be made clear in Section 2) and ii) the infinite dimensionality of the parameter space due to the latent Gaussian process component. These two issues arise in several classes of statistical models nowadays (see, for example, Beskos et al., 2006; Gonçalves and Gamerman, 2018; Gonçalves et al., 2017) and, given the high complexity

involved, it is common to find solutions in the literature which are based on discretisation of continuous processes (see, for example, Møller et al., 1998; Hildeman et al., 2018). The use of such approximations, however, has considerable disadvantages (see Simpson et al., 2016). It induces a bias in the estimates, which is typically hard to quantify and/or control. Furthermore, even if limiting results guarantee some type of convergence to the continuous model when the discretisation gets finer, the computational cost involved to get reasonably good approximations may be too high. Finally, discrete approximations may lead to serious model mischaracterisation, compromising the desired properties of the model.

The exact inference methodology proposed in this paper makes use of a simulation technique called retrospective sampling which basically allows to deal with infinite-dimensional random variables by unveiling only a finite-dimensional representation of this. A pseudo-marginal MCMC algorithm that converges to the exact posterior distribution of all the unknown quantities of the model is proposed. These quantities include the intensity function and the random partition that defines the piecewise constant structure. Also, the Monte Carlo approach makes it straightforward to sample from the predictive distribution of various appealing functions. Finally, the known high computational cost involved in algorithms that deal with the simulation of Gaussian processes is alleviated by the fact that truncated covariance functions (that zeros the covariance above a certain distance) can be used and still lead to good results. An example with 2313 observations is presented in Section 5.

Hildeman et al. (2018) also consider level-set Cox models but actually work with discretised versions of the processes. The authors consider the discretisation of compact regions in \mathbb{R}^2 based on a regular lattice and define a model on the number of observations in each subregion as conditionally (on the respective rates) independent Poisson distributions. The authors mention that “the information on the fine-scale behavior of the point pattern is lost” and define the rate in each subregion using the center point. Although the authors provide results to establish that the posterior distribution based on the discretisation converges (in total variation distance) to the posterior distribution under the continuous model, no bounds for the approximation error are provided.

Unidimensional Cox processes with piecewise constant IF have already been proposed in the literature by assuming that the IF follows a continuous time Markov chain. These are called Markov modulated Poisson processes and an efficient and exact solution to perform Bayesian inference is proposed in Rao and Teh (2013).

This paper also presents an extension of the proposed methodology to consider spatiotemporal models. This means that the point process is observed on the same region over discrete time and a temporal correlation structure is introduced in the model to explain the evolution of both the space partition and the IF levels.

Section 2 of the paper presents the level-set Cox process model and discusses its most important properties. The proposed MCMC algorithm and the extension to consider spatiotemporal models is presented in Section 3, which also addresses some relevant computational issues. Section 4 explores some simulated examples to discuss important aspects and investigate the efficiency of the proposed methodology. Finally, Section 5 applies the methodology to some real datasets. For one of them, results are compared to those obtained with a continuously varying IF Cox process model.

2 Level-set Cox process models

Let $Y = \{Y(s) : s \in S\}$ be a Poisson process in some compact region $S \in \mathbb{R}^n$ with intensity function $\lambda_S = \{\lambda(s) : s \in S\}$, $\lambda(s) : S \rightarrow \mathbb{R}^+$ and define $\mathbf{S}_K = \{S_1, \dots, S_K\}$, $K \in \mathbb{N}$, to be a finite partition of S . We shall focus on the case where $S \subset \mathbb{R}^2$ given its practical appealing, although all the definitions and results to be presented in this paper are valid for \mathbb{R}^n or any other measurable space (see Kingman, 1993). Now let $\lambda = (\lambda_1, \dots, \lambda_K)$ be a vector of positive parameters such that the IF of Y on S_k is λ_k , $k = 1, \dots, K$. Let also $c = (c_1, \dots, c_{K-1}) \in \mathbb{R}^{K-1}$, $-\infty = c_0 < c_1 < \dots < c_{K-1} < c_K = \infty$, be the values that define the level sets of a latent Gaussian process β on S and, consequently, the finite partition \mathbf{S}_K of S . The level-set Cox process model is then defined as follows:

$$(Y|\lambda_S) \sim PP(\lambda_S), \quad (1)$$

$$\lambda(s) = \sum_{k=1}^K \lambda_k I_k(s), \quad s \in S, \quad (2)$$

$$S_k = \{s \in S; c_{k-1} < \beta(s) < c_k\}, \quad k = 1, \dots, K, \quad (3)$$

$$\beta \sim GP(\mu, \Sigma(\sigma^2, \tau^2)), \quad (4)$$

$$c \sim \text{prior} \quad (5)$$

$$\lambda_k \stackrel{\text{ind}}{\sim} \text{Gamma}(\alpha_k, \gamma_k), \quad k = 1, \dots, K, \quad (6)$$

where $I_k(s)$ is the indicator of $\{s \in S_k\}$ and $GP(\mu, \Sigma(\sigma^2, \tau^2))$ is a stationary Gaussian process with mean μ and covariance function $\Sigma(\sigma^2, \tau^2)$, where σ^2 is the stationary variance and τ^2 is a range parameter indexing the correlation function. Note that the levels of the IF are not a function of the GP, which simply specifies, along with c , the partition of S that defines the piecewise constant structure. Finally, β , c and the λ_k 's are assumed to be independent *a priori*.

Notice that the likelihood of the proposed level-set Cox process model is not identifiable. That is because for each point in the (infinite-dimensional) parameter space, there are an uncountable number of other points that return the same likelihood value. That is basically implied by the non identification of the scale of the GP β . In other to see that, let us redefine β as $\beta = \mu + \sigma\beta^*$, where $\beta^* \sim N(0, \Sigma(1, \tau^2))$. Then, any transformation of the type $\mu^* = a\mu + b$, $\sigma^* = a\sigma$ and $c_k^* = b + ac_k$, $\forall m \in \mathbb{R}$, $a \in \mathbb{R}^+$, $\forall k$, defines the same partition \mathbf{S}_K and, consequently, the same likelihood value. A simple way to solve this problem and not compromise the flexibility of the model is to fix either c or the hyperparameters (μ, σ^2) . We shall adopt the latter, which also avoids the high complexity involved in estimating those parameters.

Model identifiability could also be compromised, in theory and specially when $K = 2$, by label-switching of the coordinates of λ . Nevertheless, given the complexity of the sample space, this is not expected to happen in an MCMC context, as it was the case for all the examples to be presented in this paper.

A theoretical limitation of the model is the neighboring structure implied by the continuity of the latent Gaussian process. For any model with $K \geq 3$, subregions 1 and K share a border with only one other subregion, 2 and $K - 1$, respectively, and any other subregion k shares a border with subregions $k - 1$ and $k + 1$. Whilst this represents a clear theoretical limitation of the model, it is not expected to be a practical problem in most cases. That

is because the uncertainty around the borders is higher than the uncertainty away from them, so that the need to pass through a third subregion to change between two other ones should typically not affect the model fitting and results. Furthermore, the estimated ordering of the λ_k 's will consider the likelihood of the different neighboring configurations. Figure 2 shows an example of a neighboring structure with $K = 3$ that is not contemplated by the proposed model and three possible structures that may be estimated. Despite this restriction, we highlight the great flexibility of the model to define the partition \mathbf{S}_K of S . Basically, given the neighboring restriction described above, any smooth partition of the space is contemplated by the model. In particular, it is possible to have disjoint subregions with the same IF.

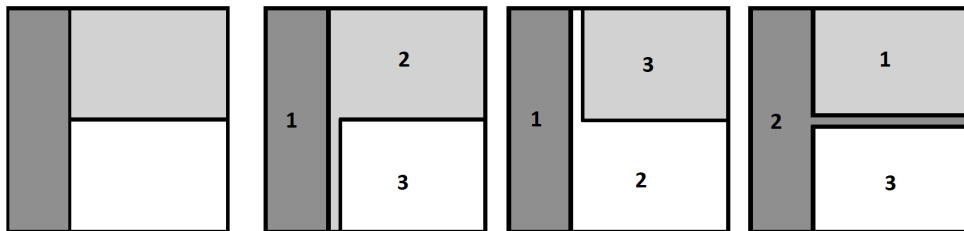


Figure 2: Example of a neighboring structure with $K = 3$ that is not contemplated by the proposed model (far left) and three possible structures that may be estimated.

We consider the number of levels K for the IF to be fixed. The choice of this value may be based on prior information about the phenomenon, the type of structure the researcher wants to estimate or even some empirical analysis of the data, for example, based on Kernel smoothing estimates of the IF (see Rowlingson et al., 2012). The choice of K should consider the trade-off between fitting and parsimony and take into account the scale of the Poisson distribution.

Finally, the piecewise constant structure allows for the analysis to be performed under a cluster analysis perspective. This may be quite useful and interpretable in some applications. Each subregion S_k constitutes a cluster and the clustering structure may be related to some practical aspect of the problem.

3 Bayesian inference

Inference for the level-set Cox process model is performed under the Bayesian paradigm, meaning that it is based on the posterior distribution of all the unknown quantities of the model. As it was mentioned before, the stationary mean and variance of the Gaussian process are fixed to identify the model. We also choose to fix the correlation parameter τ^2 . We believe this can be done in a reasonable way based on the scale of the domain S - this issue will be explored in the simulated studies in Section 4. Also, fixing the parameters that index the GP bring huge computational gains to the inference process. Regarding parameter c , we set a uniform improper prior with the restriction $c_1 < \dots < c_{K-1}$.

Defining $\theta = \{\lambda, c, \beta\}$ as all the unknown quantities of the model, the likelihood function for the level-set Cox process model is obtained by writing the density of Y w.r.t. the measure

of a unit intensity Poisson process on S (see Gonçalves and Franklin, 2019) and is given by

$$L(\theta; Y) \propto \exp \left\{ - \sum_{k=1}^K \lambda_k \mu_k \right\} \prod_{k=1}^K (\lambda_k)^{|Y_k|}, \quad (7)$$

where μ_k is the area of S_k and $|Y_k|$ is the number of events from Y on S_k .

The posterior distribution of θ as well as the full conditional distribution of any of its components have densities proportional to the joint density of (Y, θ) , which is given by

$$\begin{aligned} \pi(\theta, Y) &= L(\theta, Y) \pi(\theta) \\ &\propto \exp \left\{ - \sum_{k=1}^K \lambda_k \mu_k \right\} \left[\prod_{k=1}^K (\lambda_k)^{|Y_k|} \pi(\lambda_k) \right] \left[\prod_{k=1}^{K-1} \pi(c_k) I_{(c_1 < \dots < c_{k-1})} \right] \pi_{PG}(\beta), \end{aligned} \quad (8)$$

where $\pi_{PG}(\beta)$ is written w.r.t. some suitable dominating measure, which is irrelevant for the derivation of the inference methodology.

Given its complexity, the posterior distribution of θ is assessed via MCMC. Note, however, that there are two important issues that make the derivation of a valid and efficient algorithm not at all trivial. First, this is an infinite-dimensional MCMC, given the infinite-dimensionality of the coordinate β . Second, the likelihood in (7) is analytically intractable, since the areas μ_k of the subregions S_k cannot be computed exactly. The great challenge here is to devise a valid and efficient MCMC that is exact, i.e., that converges to the exact posterior distribution of θ , despite those two complicating issues.

In order to deal with the infinite-dimensionality of β we resort to a simulation technique called retrospective sampling. In the context of simulation of infinite-dimensional random variables, this means that only a finite-dimensional representation of the infinite-dimensional r.v. is simulated and this representation has the following two properties: i) it is enough to unveil only this representation in order to execute the algorithm in context (an MCMC in our case); ii) any finite-dimensional part of the infinite-dimensional remainder of that r.v. can be simulated conditional on this representation. This means that the GP β is to be simulated only at a finite (but random) collection of locations on each iteration of the MCMC chain. It is the particular random structure of those locations that guarantee the two properties above. The idea of retrospective sampling in the context of simulation of infinite-dimensional r.v.'s was introduced in Beskos and Roberts (2005) to perform exact simulation of diffusion paths. It was later used in a statistical context in several works (see, for example, Beskos et al., 2006; Gonçalves and Gamerman, 2018; Gonçalves et al., 2017).

The intractability of the likelihood function precludes us from performing standard Metropolis-Hastings (MH) steps for any coordinate of the chain, since all of them appear in this function. Our solution resort to a powerful and flexible general MCMC algorithm called the pseudo-marginal Metropolis-Hastings (PMMH), proposed in Andrieu and Roberts (2009). This algorithm basically allows us to replace the likelihood terms in the expression of the MH acceptance probability by a pointwise unbiased and almost surely non-negative estimator of the likelihood function. This leads to an augmented Markov chain that has the desired posterior distribution as the marginal invariant distribution of the chain - marginalised w.r.t. the random seed of the aforementioned unbiased estimator. Naturally, the efficiency of the algorithm relies on the properties of that estimator. Roughly speaking, the smaller is its variance the better (see Andrieu and Vihola, 2015).

The only unknown quantities in the expression of the likelihood function in (7) are the areas μ_k . This means that, in order to obtain an unbiased estimator for the likelihood, we need an unbiased estimator for $M = \exp \left\{ - \sum_{k=1}^K \lambda_k \mu_k \right\}$. Note that this quantity does not depend on the observed Poisson process events. Although unbiased estimators for the μ_k 's can be easily obtained using uniform r.v.'s on S , it is not straightforward to devise an unbiased estimator for M from this. We resort to a neat class of unbiased estimators called the Poisson estimator (see Beskos et al., 2006), which basically devises an unbiased estimator for M as a function of a random Poisson number of uniformly distributed r.v.'s on S . The unbiased estimator for M and some of its important properties are given in Propositions 1 and 2, respectively.

Proposition 1. *An unbiased and almost surely positive estimator for M is given by*

$$\hat{M} = e^{-\mu(S)\lambda_m} \prod_{k=1}^K \left(\frac{\delta\lambda_M - \lambda_k}{\delta\lambda_M - \lambda_m} \right)^{|N_k|}, \quad (9)$$

where $\delta > 1$, $N = g(N^*, \lambda^*)$, $\lambda^* = (\delta\lambda_M - \lambda_m)$, $\lambda_M = \max_k \{\lambda_k\}$, $\lambda_m = \min_k \{\lambda_k\}$ and $\mu(S)$ is the area of S . N^* is a unit intensity Poisson process in the cylinder with base S and height from 0 to $+\infty$. Function g is the projection, in S , of the points from N^* that have height smaller than λ^* . As a consequence, N is a homogeneous Poisson process on S with intensity λ^* . Finally, $|N_k|$ is the number of points from N falling on S_k .

Proposition 2. *Estimator \hat{M} has a finite variance which is a decreasing function of δ .*

Proof. See Appendix A for the proofs of Propositions 1 and 2. \square

In our retrospective sampling context, it is N that determines the locations at which β is to be simulated, besides the locations from Y . Furthermore, the mean number of locations from N is $(\delta\lambda_M - \lambda_m)\mu(S)$, which gives the intuition for the result in Proposition 2. This establishes a trade-off related to the choice of δ , as an increase in its value reduces the variance of \hat{M} (and consequently improves the mixing of the MCMC chain) but increases the computational cost of the MCMC algorithm (and vice-versa).

We define a pseudo-marginal MCMC algorithm to sample from the posterior distribution of θ based on the estimator in (9). On each iteration of the Markov chain, the general algorithm proposes a move $(\theta, N^*) \rightarrow (\tilde{\theta}, \tilde{N}^*)$ from a density $q(\tilde{\theta}, \tilde{N}^* | \theta, N^*) = q(\tilde{\theta} | \theta) q(\tilde{N}^* | N^*)$, where $q(\tilde{N}^* | N^*) = q(\tilde{N}^*)$ is the Poisson process prior defined in Proposition 1, and accepts with probability given by

$$1 \wedge \frac{\hat{\pi}(\tilde{\theta}; \tilde{N}^*) q(\theta | \tilde{\theta})}{\hat{\pi}(\theta; N^*) q(\tilde{\theta} | \theta)}, \quad (10)$$

where

$$\hat{\pi}(\theta; N^*) = e^{-\mu(S)\lambda_m} \left[\prod_{k=1}^K \left(\frac{\delta\lambda_M - \lambda_k}{\delta\lambda_M - \lambda_m} \right)^{|N_k|} (\lambda_k)^{|Y_k|} \pi(\lambda_k) \right] \pi(c) \pi_{PG}(\beta). \quad (11)$$

The algorithm above is bound to be inefficient as it is, given the complexity of the chain's coordinates. We adopt simple yet important changes to obtain a reasonably efficient

algorithm. First, we split the coordinates in blocks, making this a Gibbs sampling with pseudo-marginal MH steps. This implies that the acceptance probability of any block is also given by (10). Also, the choice to define N as a function of N^* , with the distribution of the latter being independent of θ , instead of working directly with N , allows us to sample N^* alone as one block of the Gibbs sampler. Furthermore, note that N^* has an infinite collection of points but, in order to evaluate the acceptance probability in (10), it is enough to unveil N - the projection on S of the points of N^* that are below λ^* . This means that, as it is the case for β , N^* is also sampled retrospectively. The blocks of the Gibbs sampling are: N^* , β , λ , c . The algorithm to sample from each block is described below.

3.1 Sampling N^*

The standard version of the pseudo-marginal algorithm proposes a move in N^* from its prior Poisson process distribution, which is accepted with probability given by (10). Furthermore, the fact that the acceptance probability in (10) depends on N^* only through the points falling below λ^* , implies that we only need to unveil N in order to update N^* . Nevertheless, since N^* will typically have many points falling below λ^* , this proposal might have a low acceptance rate which, in turn, may compromise the mixing of the chain.

Instead, we adopt a proposal distribution that updates N^* below and above λ^* separately. The latter is proposed from the prior and accepted with probability 1, given that it does not appear in (10). For that reason, this step is only performed conceptually and points from N^* above λ^* are sampled retrospectively, if required (when the proposal value for λ leads to a higher value of λ^*), from a $PP(1)$. For the points below λ^* , we adopt a proposal distribution that is invariant w.r.t. the prior of N^* in that region, i.e., a unit rate Poisson process in the cylinder under λ^* and, therefore, preserves the acceptance probability in (10). The proposal consists of three possible moves: i) add a point uniformly distributed in the cylinder; ii) remove a point uniformly chosen among the existing ones; iii) preserve the current points. Each of these three moves are proposed with a suitable probability that preserves the PP prior of N^* as its invariant distribution.

However, this is still not an efficient proposal because the moves are possibly too “small” in terms of the number of points of N^* below λ^* . We resolve this issue by splitting S into L regular squares (assuming that S is a rectangle) and updating N^* in each of the respective cylinders separately and using the ± 1 discrete random walk proposal described above. This strategy imposes an optimal scaling problem w.r.t. L . The existing 0.234 optimal acceptance rate result (see Roberts et al., 1997) may not be suitable here as this rate is likely to be achieved for a value of L that yields a small mean number of points in each square and, therefore, it is not suitable to apply Central Limit Theorem results. Empirical analyses for several simulated examples (some of which are presented in Section 4) suggest that the value of L should be chosen so that the average acceptance rate over the L squares is between 0.75 and 0.8.

For each of the L squares, the proposal distribution has the following probabilities:

$$\begin{aligned}
 q(n, n+1) &= \frac{A}{A+n+1}; \\
 q(n, n-1) &= \begin{cases} \frac{n}{A+n}, & \text{if } n > 0; \\ 0, & \text{if } n = 0; \end{cases} \quad (12)
 \end{aligned}$$

$$q(n, n) = 1 - (q(n, n + 1) + q(n, n - 1)),$$

where n is the current number of points in that square and $A = \lambda^* \mu(S)/L$. Simple calculations show that a $Poisson(A)$ distribution is reversible for the Markov chain defined by the probabilities in (12). The invariance w.r.t a $PP(1)$ is guaranteed by the continuous and discrete uniform distributions adopted to add and remove a point, respectively. Cancellation of terms in the expression of the acceptance probability in (10)-(11) implies that the acceptance probability of a move in each of the L squares is

$$\alpha_{N^*} = \begin{cases} \frac{\delta\lambda_M - \lambda_k}{\delta\lambda_M - \lambda_m}, & \text{if the proposal adds a point on } S_k; \\ 1, & \text{otherwise.} \end{cases} \quad (13)$$

3.2 Sampling β

The latent process β is sampled retrospectively, due to its infinite dimensionality. This means that it is sampled at a finite collection of locations which are enough to perform all the steps of the MCMC algorithm. This collection is defined by the locations of Y and N , with the latter changing along the MCMC on the update steps of N^* and λ .

We adopt the prior GP as the proposal distribution for β as this cancels the $\pi_{PG}(\cdot)$ terms in the expression (10) of the acceptance probability. This proposal, however, is independent and is bound to lead to a small acceptance rate. This problem is mitigated by choosing, on each iteration of the Gibbs sampler, a finite set of locations at which β is not updated. This set is a fixed proportion p_N of the locations of N that is uniformly chosen on every iteration. The proposal is now simulated from the prior GP conditional on the value of β at those locations. This strategy poses an optimal scaling problem related to the choice of p_N such that the infinite dimensionality of β and the similarity between this proposal distribution and a random walk suggest that p_N should be chosen so to have an acceptance rate of approximately 0.234 (see Roberts et al., 1997).

The acceptance probability of a move $\beta \rightarrow \check{\beta}$ is given by

$$\alpha_\beta = 1 \wedge \prod_{k=1}^K \left(\frac{\delta\lambda_M - \lambda_k}{\delta\lambda_M - \lambda_m} \right)^{|\check{N}_k| - |N_k|} (\lambda_k)^{|\check{Y}_k| - |Y_k|}, \quad (14)$$

where $|N_k|$ and $|Y_k|$ are the respective values obtained from β and $|\check{N}_k|$ and $|\check{Y}_k|$ are the respective values obtained from $\check{\beta}$.

3.3 Sampling λ and c

The vector λ is sampled jointly from a proposal given by a Gaussian random walk with a properly tuned covariance matrix that is adapted, based on the respective empirical covariance matrix of the chain, up to a certain iteration (see Roberts and Rosenthal, 2009) so to have the desired acceptance rate - varying from 0.4 to 0.234 according to the dimension of λ . The acceptance probability of a move $\lambda \rightarrow \check{\lambda}$ is given by

$$\alpha_\lambda = 1 \wedge e^{-\mu(S)(\ddot{\lambda}_m - \lambda_m)} \prod_{k=1}^K \frac{\left(\frac{\delta \ddot{\lambda}_M - \ddot{\lambda}_k}{\delta \lambda_M - \lambda_m}\right)^{|\ddot{N}_k|}}{\left(\frac{\delta \lambda_M - \lambda_k}{\delta \lambda_M - \lambda_m}\right)^{|N_k|}} \left(\frac{\ddot{\lambda}_k}{\lambda_k}\right)^{|Y_k| + \alpha_k - 1} e^{-\gamma_k(\ddot{\lambda}_k - \lambda_k)}, \quad (15)$$

where \ddot{N}_k is the respective value obtained from $\ddot{N} = g(N^*, \ddot{\lambda}^*)$ and $\ddot{\lambda}^* = (\delta \ddot{\lambda}_M - \ddot{\lambda}_m)$.

The parameter vector c is jointly sampled from a uniform random walk proposal with a common (and properly tuned) length for each of its components. If the ordering of the proposed values is preserved, a move $c \rightarrow \ddot{c}$ is accepted with probability

$$\alpha_c = 1 \wedge \left[\prod_{k=1}^K \left(\frac{\delta \lambda_M - \lambda_k}{\delta \lambda_M - \lambda_m}\right)^{|\ddot{N}_k| - |N_k|} \right], \quad (16)$$

where \ddot{N}_k is the respective value obtained from the S_k subregion defined by \ddot{c} .

3.4 Computational aspects

3.4.1 Computational cost of the Gaussian process

The computational bottleneck of the proposed MCMC algorithm is the sampling of the Gaussian process β , which is performed not only when updating this component but also, retrospectively, when updating N^* and λ . The cost to simulate from a d -dimensional multivariate normal distribution is $\mathcal{O}(d^3)$ and, in our case, $d = |Y| + |N|$, which is a typically high value (in the order of 10^3). Several solutions have been proposed in the literature to deal with this problem. Some of them are exact in the sense that the approximation process defines a valid probability measure (see, for example Datta et al., 2016). This property is highly desirable as the validity of the Bayesian paradigm is preserved. We resort to an exact approximation that sets the correlations to be zero for distances larger than a specified threshold. This may have a considerable negative impact in contexts in which the model being considered has a direct strong dependence on the GP, for example, in geostatistical models in which the GP is observed or in Cox process in which the IF is a continuous function of the GP, as in Gonçalves and Gamerman (2018). In our case, however, the GP is used only to determine the partition of S , but not the actual values of the IF. Therefore, it is reasonable to expect that the efficiency of our methodology is not compromised when using this (exact) approximation. This approach leads to considerable gains in terms of computational cost, allowing for the proposed methodology to be applied to reasonably sized datasets.

In this paper, we shall adopt the following covariance function for the GP prior of β . Given a threshold $r > 0$,

$$\text{cov}(\beta(s), \beta(s')) = \begin{cases} \sigma^2 \exp\left\{-\frac{1}{2\tau^2}|s - s'|^\gamma\right\}, & \text{if } |s - s'| \leq r, \\ 0, & \text{if } |s - s'| > r, \end{cases} \quad (17)$$

for $s, s' \in S$, where $|s - s'|$ is the distance between s and s' . The fact that the non-truncated covariance function is a valid one implies that the truncated version also is and, in turn, also is the resulting GP measure.

As it has been mentioned before, the hyperparameters indexing the GP will be fixed. We set $\mu = 0$ and $\sigma^2 = 1$. The values of τ^2 , γ and r are chosen based on the scale of S .

As a default, we consider 10x10 square regions and set $\gamma = 3/2$. Different values of τ^2 and r are compared in the simulations presented in Section 4. We consider values of r varying from 3.5% to 9% of the maximum distance ($10\sqrt{2}$) in S and values 0.7, 2 and 5 for τ^2 . Results suggest that $r = 1$ and $\tau^2 = 5$ are a reasonable and robust choice (see Section 4 for details).

3.4.2 MCMC virtual updates

Despite the strategy described above, the computational cost of the MCMC algorithm may still be compromised by a large accumulation of points from β resulted from successive rejections on the update step of this component and the simulation of extra points on the update steps of λ and N^* .

The infinite dimensionality of β and the retrospective sampling strategy provide an elegant and efficient solution for this problem. We add virtual update steps to the MCMC algorithm that update β in $S \setminus \{Y, N\}$. Since the acceptance probability (10) of the pseudo-marginal algorithm does not depend on β at those locations, the proposal is accepted with probability 1. Furthermore, the retrospective sampling approach implies that, in fact, those steps consist of simply deleting all the stored values of β at $S \setminus \{Y, N\}$, justifying the term “virtual” step. A virtual update is performed in-between every block update of the Gibbs sampling as long as the set of sampled locations of β in $S \setminus \{Y, N\}$ is not empty at that moment of the algorithm.

3.4.3 Other important issues

The choice of the initial values of the MCMC algorithm plays an important role to determine the efficiency of the algorithm. Results from simulation studies suggest that the convergence of the MCMC algorithm is considerably improved for reasonable choices of the initial values, as the following one. The initial partition \mathbf{S}_K is chosen based on an empirical analysis of the data that may include the estimation of the IF via Kernel smoothing (see Rowlingson et al., 2012). The initial values of β and c are set considering the scale of the GP prior, i.e., mean 0 and variance 1, such that β is set to be constant inside each subregion S_k . Finally, we set all the λ_k 's to be $\frac{|Y|}{\mu(S)}$ and simulate $N \sim PP(\lambda^*)$.

Although the explicit identifiability problems of the likelihood function described in Section 2 are solved by fixing the parameters of the Gaussian process prior, local modes in the posterior density may still exist, in particular, in examples with a high concentration of point in small regions. This is an intrinsic problem when performing inference for Cox processes due to the ill behaved likelihood function. It is straightforward to see that the likelihood is maximised when the IF is zero in $S \setminus Y$ and increases indefinitely as the value of the IF at Y increases. Therefore, the prior on the IF regularises the problem and, consequently, has a great impact on the posterior distribution. In this sense, the prior information may not be enough to avoid the existence of significant local modes. This issue is illustrated for one of the applications presented in Section 5.1. More specifically, we show that different initial values of the MCMC lead to considerably different posterior samples.

It is reasonable to expect that the data are not highly informative about parameters c and, therefore, the inference process should not be harmed, in many cases, if c is fixed at suitable values. In this case, the values of c should be chosen based on the scale of the GP and the choice for K . For example, the values of c could be chosen so to split the real

line into K intervals of equal probability under the marginal stationary distribution of the GP prior - $N(0, 1)$. Results from the simulation studies in Section 4 suggest that this is a reasonable choice.

The choice of δ is also investigated in the simulation studies in Section 4 under the trade-off defined by the fact that an increase in δ improves the mixing of the MCMC algorithm but also increases its computational cost. Simulations indicate that the distribution of the pseudo-marginal estimator has a very heavy tail to the right and that a choice of δ based on the mean number of points of N is reasonably robust among different models. In particular, results were good for a variety of examples (some of which are presented in Section 4.1) when that mean number of points from N was around 5000.

Finally, parameter λ is expected to be strongly affected by the variance of the pseudo-marginal estimator and, therefore, it makes sense to perform multiple updates of this parameter at each iteration of the Gibbs sampling. For the examples presented in this paper, 30 updates per iteration were performed.

Considering all the algorithms and issues described in this section, the MCMC algorithm to sample from the posterior distribution for the level-set Cox process model is as presented in Appendix B.

3.5 Spatiotemporal extension

The level-set Cox process model proposed in Section 2 can be extended to a spatiotemporal context such that the data can be seen as a time series of point processes in a common space S in discrete time. The temporal dependence is defined by a spatiotemporal Gaussian process and, possibly, a temporal structure for the level parameters of the IF. Conditional on those components, the observed Poisson process is independent among different times.

Suppose that the point process Y is observed at $T + 1$ times - $0, \dots, T$, where $Y_t = \{Y_t(s) : s \in S\}$ is a Poisson process with IF $\lambda_{t,S} = \{\lambda_t(s) : s \in S\}$. For each time t , we define a finite partition $\mathbf{S}_{t,K} = \{S_{t1}, \dots, S_{tK}\}$, $K \in \mathbb{N}$, of S and a sequence $c = (c_1, \dots, c_{K-1}) \in \mathbb{R}^{K-1}$, with $-\infty = c_0 < c_1 < \dots < c_{K-1} < c_K = \infty$. The spatiotemporal model is defined as follows.

$$(Y_t | \lambda_{t,S}) \stackrel{ind.}{\sim} PP(\lambda_{t,S}), \quad t = 0, \dots, T, \quad (18)$$

$$\lambda_t(s) = \sum_{k=1}^K \lambda_{tk} I_{tk}(s), \quad s \in S, \quad t = 0, \dots, T, \quad (19)$$

$$S_{tk} = \{s \in S; c_{k-1} < \beta_t(s) < c_k\}, \quad k = 1, \dots, K, \quad t = 0, \dots, T, \quad (20)$$

$$\beta = (\beta_0, \dots, \beta_T) \sim DGP(\mu, \Sigma(\sigma^2, \tau^2), \Sigma(\xi^2, \varrho^2)), \quad (21)$$

$$c \sim \text{prior} \quad (22)$$

$$\lambda_k = (\lambda_{0k}, \dots, \lambda_{Tk}) \stackrel{ind.}{\sim} NGAR1(a_{0k}, b_{0k}, w_k, a_k), \quad k = 1, \dots, K, \quad (23)$$

where $I_{tk}(s)$ is the indicator of $\{s \in S_{tk}\}$, DGP is a dynamic Gaussian process (see Gamerman, 2010) and $NGAR1$ is an order 1 non-Gaussian non-linear autoregressive model. We consider a DGP of the form:

$$\beta_0 \sim GP(\mu, \Sigma(\sigma^2, \tau^2)), \quad (24)$$

$$\beta_t(s) = \beta_{t-1}(s) + \zeta_t(s), \quad s \in S, \quad t = 1, \dots, T, \quad (25)$$

$$\zeta_t \sim GP(0, \Sigma(\xi^2, \varrho^2)). \quad (26)$$

As in the case of the spatial model, we set $\mu = 0$, $\sigma^2 = 1$ and fix τ^2 at a suitable value. Parameters ξ^2 and ϱ^2 are also fixed such that $\xi^2 < \sigma^2$ and $\varrho^2 \geq \tau^2$. Now, for each k , we define the following *NGAR1* model.

$$\lambda_{0k} \sim \text{Gamma}(a_{0k}, b_{0k}), \quad (27)$$

$$\lambda_{tk} = w_k^{-1} \lambda_{t-1k} \varsigma_{kt}, \quad t = 1, \dots, T, \quad (28)$$

$$\varsigma_t \sim \text{Beta}(w_k a_k, (1 - w_k) a_k). \quad (29)$$

where parameters a_{0k} , b_{0k} , w_k and a_k are fixed at suitable values. This *NGAR1* model imposes a random walk type structure to the logarithm of λ_{tk} and is inspired by the non-Gaussian state space model proposed in Smith and Miller (1986).

A temporal structure can be considered to model both the random partitions and the levels of the IF as in the model above or to model only the former, in which case the λ_{tk} parameters are all independent with gamma priors.

3.5.1 Inference for the spatiotemporal model

Inference for the spatiotemporal level-sex Cox process model above requires some adaptations to the MCMC algorithm proposed for the spatial model. First, we need to define one pseudo-marginal estimator for the likelihood of Y in each time t and we shall define the respective auxiliary variables as $N^* = (N_0^*, \dots, N_T^*)$. Now, each N_t^* is an independent unit rate Poisson process on the infinite height cylinder with base S and $N_t = g(N_t^*, \lambda_t^*)$, $\lambda_t^* = (\delta_t \lambda_{tM} - \lambda_{tm})$, $\lambda_{tM} = \max_k \{\lambda_{tk}\}$ and $\lambda_{tm} = \min_k \{\lambda_{tk}\}$. Furthermore, whenever β is to be sampled retrospectively on the update steps of the λ_k 's and N^* , it is sampled from the spatiotemporal GP prior and, therefore, conditional on all the locations of β already sampled at all times 0 to T .

The sampling step of N^* is performed analogously to the spatial case at each time t , independently. Parameter c uses the same proposal of the spatial case and accepts a move $c \rightarrow \check{c}$ with probability

$$\alpha_c = 1 \wedge \left[\prod_{t=0}^T \prod_{k=1}^K \left(\frac{\delta_t \lambda_{tM} - \lambda_{tk}}{\delta_t \lambda_{tM} - \lambda_{tm}} \right)^{|\check{N}_{tk}| - |N_{tk}|} \right]. \quad (30)$$

The most straightforward way to sample β is to uniformly choose a fixed proportion p_{N_t} of N_t to fix the value of β_t , for all t , and propose β from its *DGP* prior. The acceptance probability of a move $\beta \rightarrow \check{\beta}$ is then given by

$$\alpha_\beta = 1 \wedge \prod_{t=0}^T \prod_{k=1}^K \left(\frac{\delta_t \lambda_{tM} - \lambda_{tk}}{\delta_t \lambda_{tM} - \lambda_{tm}} \right)^{|\check{N}_{tk}| - |N_{tk}|} (\lambda_{tk})^{|\check{Y}_{tk}| - |Y_{tk}|}. \quad (31)$$

The computational cost of this step may be too high and, as an alternative, β can be sampled in blocks of times.

Finally, if no temporal dependence structure is considered for the λ_k 's, the same algorithm from the spatial model is considered independently at each time t to sample $(\lambda_{t1}, \dots, \lambda_{tK})$. If, however, the *NGAR1* prior is adopted, the λ_k 's are jointly sampled

by proposing from a properly tuned Gaussian random walk. The respective acceptance probability is given by

$$\alpha_\lambda = 1 \wedge \left[\prod_{t=0}^T e^{-\mu(S)(\ddot{\lambda}_{tm} - \lambda_{tm})} \prod_{k=1}^K \frac{\left(\frac{\delta_t \ddot{\lambda}_{tM} - \ddot{\lambda}_{tk}}{\delta_t \ddot{\lambda}_{tM} - \ddot{\lambda}_{tm}} \right)^{|\ddot{N}_{tk}|}}{\left(\frac{\delta_t \lambda_{tM} - \lambda_{tk}}{\delta_t \lambda_{tM} - \lambda_{tm}} \right)^{|N_{tk}|}} \left(\frac{\ddot{\lambda}_{tk}}{\lambda_{tk}} \right)^{|Y_{tk}|} \right] \prod_{k=1}^K \frac{\pi(\ddot{\lambda}_k)}{\pi(\lambda_k)}, \quad (32)$$

where $\pi(\lambda_k)$ is the density of the *NGAR1* prior.

3.6 Prediction

It is often the case that the analysis of point process phenomena also aims at predicting unknown quantities conditional on the data. In the spatial context, this may include the some functional of the IF in a given subregion of S or future replications of the observed process. In the spatiotemporal context, prediction about future times may be considered. In both cases, it is straightforward to obtain a sample from the desired predictive distribution based on the output of the MCMC.

The algorithm to sample from the predictive distribution of a function $h(\lambda_S)$ under the spatial model consists of computing $h(\lambda_S)$ for each sampled value of λ_S in the MCMC chain (after a suitable burn-in). If $h(\lambda_S)$ is intractable it may still be possible to obtain a sample from the predictive distribution of a unbiased estimator of $h(\lambda_S)$. For example, define $h(\lambda_S) = \int_{S_0} \lambda(s) ds$, for some known $S_0 \subset S$, and $U \stackrel{ind.}{\sim} Unif(S_0)$. Then, an unbiased estimator of $h(\lambda_S)$ is given by (see Gonçalves and Gamerman, 2018, Section 4.3)

$$\hat{h} = \mu(S_0)\lambda(U). \quad (33)$$

A sample from the predictive distribution of (33) is obtained by sampling $U_i \sim Unif(S)$ and $\lambda(U_i)$ on each iteration of the MCMC.

In order to perform prediction for replications of Y it is enough to simulate Y conditional on each sampled value of λ_S in the MCMC using a Poisson thinning algorithm. This consist of simulating a $PP(\lambda_M)$ in S and keeping each point s with probability $\lambda(s)/\lambda_M$, where the value of $\lambda(s)$ is obtained by sampling $\beta(s)$ retrospectively from the GP prior on each MCMC iteration.

Now consider the full Bayesian model of a level-set Cox process Y in S for times $0, \dots, T, \dots, T + d$, $d \in \mathbb{N}$, and let y be a realisation of the process at times $0, \dots, T$. Define $h(Y, \lambda_d)$ to be some measurable function, in the probability space of the full Bayesian model, that depends on $(Y_t, \lambda_{t,S})$ only for times $t \in \{T + 1, \dots, T + d\}$. Then, prediction about $h(Y, \lambda_d)$ is made through the predictive distribution of $(h(Y, \lambda_d)|y)$, which is sampled by simulating $h(Y, \lambda_d)$, conditional on the output of the MCMC on each iteration, based on the following identity.

$$\pi(h(Y, \lambda_d)|y) = \int \pi(h(Y, \lambda_d)|\lambda_{0:T}, y)\pi(\lambda_{0:T}|y)d\lambda_{0:T}. \quad (34)$$

Appealing examples of $h(Y, \lambda_d)$ include:

- i. $(\lambda_{T+1,S}, \dots, \lambda_{T+d,S})$;

- ii. $\Lambda_L = \int_S \lambda_t(s) ds$, for $t = T + 1, \dots, T + d$;
- iii. $(Y_{T+1}, \dots, Y_{T+d})$.

4 Simulated examples

We perform a series of simulation studies to investigate the main issues regarding the methodology proposed in this paper. First, a sensitive analysis w.r.t. the prior correlation structure of the Gaussian process prior is presented, followed by a sensitivity analysis regarding the choice of δ . Then an analysis is presented to explore the choice of the number of levels K of the intensity function and the behavior of the posterior distribution when the true model has a neighboring structure that is not contemplated by the proposed model. All the examples presented in this paper are implemented in Ox (Doornik, 2009) and run in a i7 3.50GHz with 16GB RAM. Also, parameter c is fixed at 0, (-0.5, 0.5) and (-0.7, 0, 0.7) for $K = 2, 3$ and 4, respectively.

Throughout the analyses described above, the efficiency of the proposed methodology in terms of estimation and computational cost is investigated.

4.1 Sensitivity analyses

We consider an example with $K = 3$ and $\lambda_1 = 9$, $\lambda_2 = 4$, $\lambda_3 = 1.55$, to perform some sensitivity analysis regarding some prior specifications required by the proposed methodology. The real IF is shown in Figure 3. Note that the true partition is not allowed by the proposed model but the idea is to also illustrate how this is not a issue in practice.

The first analysis concerns the specification of the correlation structure of the Gaussian process prior through the choices of parameter τ^2 and radius r in (17). We run the MCMC algorithm for nine different specifications by crossing three values for τ^2 (0.7, 2 and 5), with three values for r (0.5, 1 and 1.25). All the scenarios consider $\delta = 5$. Comparison is performed in terms of the computational cost and estimate of the intensity function. Table 1 shows some of the results and Figure 13 in Appendix C shows the intensity function estimated in each case. Results indicate a better performance when $\tau^2 = 5$ and $r = 1$. Figure 3 shows the real IF and the posterior mean for that specification.

τ^2 / r	0.7 / 0.5	0.7 / 1	0.7 / 1.25	2 / 0.5	2 / 1	2 / 1.25	5 / 0.5	5 / 1	5 / 1.25
cost	2.591	3.968	6.296	4.131	2.014	5.787	1.951	1.009	2.960
$\lambda_1 = 9$	9.06 / 0.88	8.73 / 0.78	8.98 / 0.81	8.72 / 0.78	8.81 / 0.77	8.93 / 0.81	8.73 / 0.73	8.72 / 0.74	9.02 / 0.73
$\lambda_2 = 4$	4.20 / 0.49	3.90 / 0.44	3.95 / 0.40	4.48 / 0.63	4.14 / 0.50	3.92 / 0.45	4.60 / 0.55	4.25 / 0.49	3.87 / 0.44
$\lambda_3 = 2$	1.63 / 0.16	1.60 / 0.16	1.55 / 0.17	1.69 / 0.16	1.63 / 0.17	1.62 / 0.16	1.68 / 0.16	1.66 / 0.16	1.63 / 0.17

Table 1: Results for the sensitivity analysis regarding the specification of the correlation structure of the prior Gaussian process. Second row reports the time, in seconds, per effective sample of the pseudo-marginal log-likelihood. The remaining rows show the posterior mean and standard deviation of the λ_k parameters.

We now take the chosen specification ($\tau^2 = 5$ and $r = 1$) and compare the results for different values of δ . Given that the value of δ only affects the mixing of the MCMC and does not change the posterior distribution, comparison is made in terms of the computational

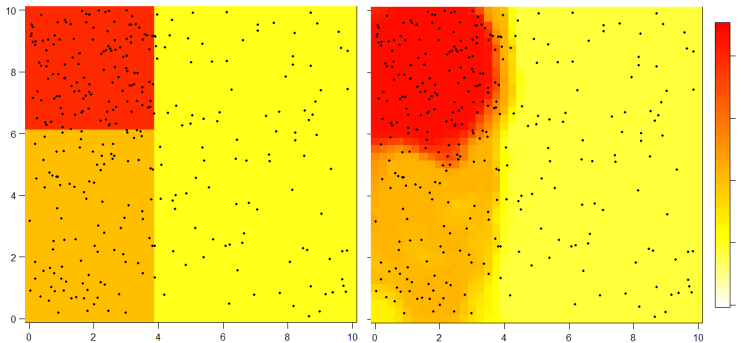


Figure 3: Real IF and its posterior mean when $\tau^2 = 5$ and $r = 1$.

cost and the results, presented in Table 2, indicate a superior performance when $\delta = 5$. This means that the average number of points from N is around 4500.

Trace plots and autocorrelation plots for the case where $\tau^2 = 5$, $r = 1$ and $\delta = 5$ are presented in Figure 11 of Appendix C material and strongly suggest the convergence of the algorithm. A different initial value for the random partition, which is not in accordance with the true IF, was used to run the algorithm and showed how it takes considerably longer for the MCMC algorithm to converge. These results are presented in Figure 12 of Appendix C.

	$\delta = 3$	$\delta = 5$	$\delta = 7$
cost	1.101	1.009	5.426

Table 2: Results for the sensitivity analysis regarding the specification of δ . Time, in seconds, per effective sample of the pseudo-marginal log-likelihood.

4.2 Model fit

We now explore the issue of choosing the number of levels K of the IF. We consider the example from the sensitivity analysis previously presented and fit the model for $K = 2, 3, 4$, with $\tau^2 = 5$, $r = 1$ and $\delta = 5$. Results are presented in Table 3 and Figure 4 and clearly indicate, as expected, that $K = 3$ is the best choice. For $K = 2$, the model estimates the two true subregions with the larger values of the IF as one region with an estimated value between the two true ones. On the other hand, when $K = 4$, the model identifies the three true subregions and estimates the two lowest levels to be very similar (1.66 and 1.57).

	$K = 2$	$K = 3$	$K = 4$
$\lambda_1 = 9$	-	8.72 / 0.74	8.58 / 0.74
$\lambda_2 = 4$	6.15 / 0.40	4.25 / 0.49	3.96 / 0.46
$\lambda_3 = 1.5$	1.60 / 0.17	1.66 / 0.16	1.66 / 0.26
λ_4	-	-	1.57 / 0.22

Table 3: Results for the sensitivity analysis regarding the specification of K . Posterior mean and standard deviation of the λ_k parameters.

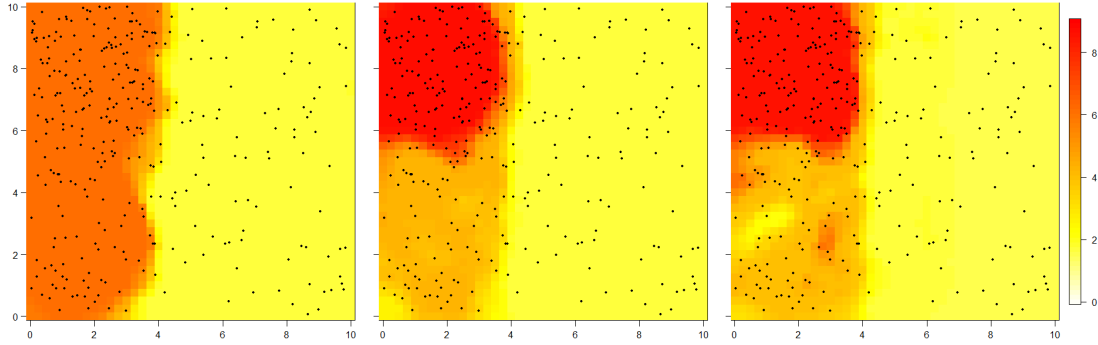


Figure 4: Estimated IF for $K = 2, 3$ and 4 .

We also fit the proposed level-set Cox process model to a dataset generated with an IF surface that is not contemplated by the neighboring structure of the proposed model. The true parameter values are $\lambda_1 = 2$, $\lambda_2 = 5$ and $\lambda_3 = 10$ and we set $\tau^2 = 5$, $r = 1$ and $\delta = 5$. The true and estimated IF are presented in Figure 5 and, as expected, the estimation is not seriously affected by the neighboring restriction. The model basically estimates a transition region where the IF passes through the middle level to go from the lowest to the highest one.

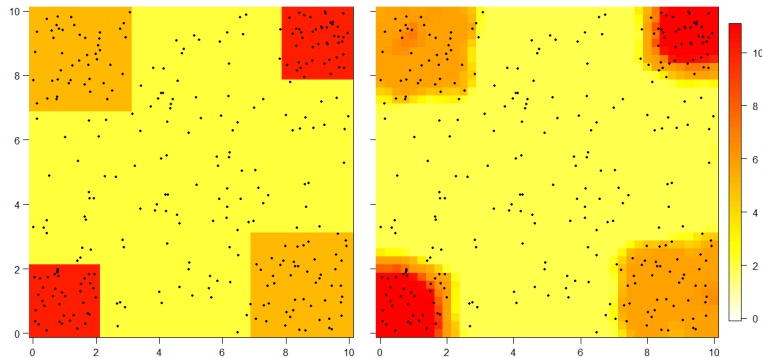


Figure 5: True and estimated IF. The posterior mean of the λ_k 's is 1.813, 5.828 and 11.040.

5 Applications

We apply the level-set Cox process model to analyse some real point process datasets. We present four applications for the spatial model. Two of them concern the location of a certain type of tree in some region, the third one considers the location of particles in a bronze filter and the fourth one considers fires in a region of New Brunswick, Canada, over 16 years. We also present a spatiotemporal example regarding the fires in New Brunswick, but segregating the data per year for the last four years in the dataset. All the datasets are available in the R package `spatstat` (Baddeley et al., 2015).

For the first example, we also present an analysis comparing the level-set Cox process model to a Cox process model in which the IF is a continuous function of a latent Gaussian process. The latter is proposed in Gonçalves and Gamerman (2018), who also present an

exact methodology to perform Bayesian inference. Their model assumes $\lambda(s) = \lambda^* \Phi(\beta(s))$, where λ^* is an unknown parameter, β is a Gaussian process and Φ is the standard normal c.d.f.

The fourth example contains 2313 observation and illustrates the scalability of the proposed methodology to be used with large datasets.

5.1 Spatial examples

We analyse a dataset regarding the location of white oak trees in Lansing Woods, Michigan. The data consists of the location of 448 white oaks in an area of 924×924 feet, which we rescale to $(0, 10) \times (0, 10)$.

An empirical analysis based on the Kernel smoothing estimation of the IF suggested that $K = 3$ would be a suitable choice. Indeed, a model with $K = 4$ was also fit and two of the levels were estimated to be quite similar (2.74, 2.22, 5.07, 7.98). Figure 6 shows the posterior mean and mode of the posterior. The latter defines the partition using its pointwise mode and colors each subregion with the posterior mean of the respective λ_k .

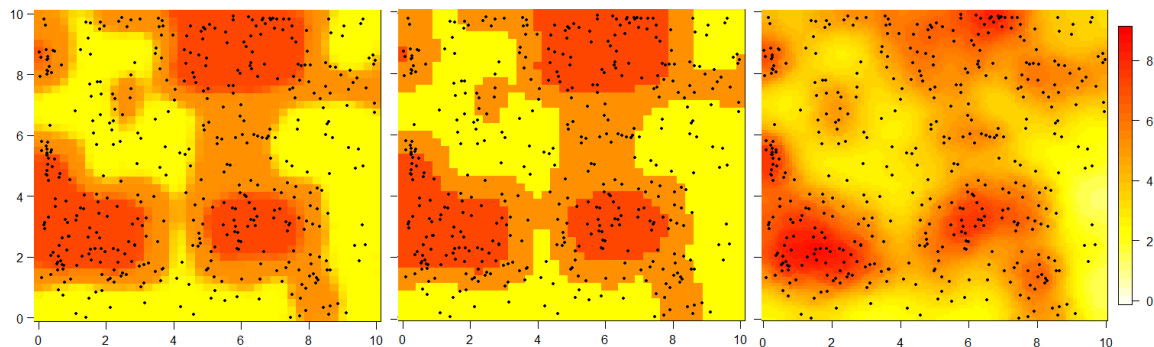


Figure 6: Posterior mean (left) and mode (middle) of the IF under the proposed model and posterior mean (right) of IF under the continuous IF model for the white oak example.

We also consider the prediction of the integrated IF in the whole observed region and in two subsets of this, $S_1 = (5, 7) \times (8, 10)$ and $S_2 = (8, 10) \times (4.5, 6.5)$. The continuous IF Cox process model from Gonçalves and Gamerman (2018) is also fit and predictions are compared. Figure 6 shows the estimated IF for both models. Predictions are presented in Table 4. Results show that more precise predictions are obtained with the level-set model (3.3% more precise for S , 76% more precise for S_1 and 174% more precise for S_2).

	$ \mathbf{Y} $	Proposed model	Continuous IF model
S	448	451.12 / 23.36	448.44 / 24.14
S_1	27	31.08 / 2.38	25.35 / 4.18
S_2	9	9.37 / 1.03	9.98 / 2.82

Table 4: Mean and variance of the predictive distribution of the estimator in (33).

The second spatial example considers the location of 584 pinus palustris trees in a 200×200 meters region in the south of Georgia. We rescale the observed region to $(0, 10) \times (0, 10)$. An empirical analysis via Kernel smoothing estimation suggested that $K = 3$. A model

with $K = 4$ was also fit and two of the levels were estimated to be quite similar (2.83, 4.12, 5.38, 10.69). In both cases the four small regions with a very high concentration of points are incorporated into a larger partition region with moderate IF. If, however, we set initial values for the MCMC chain that has four tight squares around these four regions as one partition region with a high IF value, the MCMC algorithm converges to a different configuration. This clearly indicates the presence of a local mode as discussed in Section 3.4.3, meaning that, for datasets with this behavior (of having small regions with very high concentration of points) the prior measure imposed to the IF may not be able to fully identify the posterior distribution. In this case, it depends on the user to set initial values coherent with the type of structure for the IF that he/she wants to obtain. Figure 7 shows the posterior mean and mode for both initial value configurations.

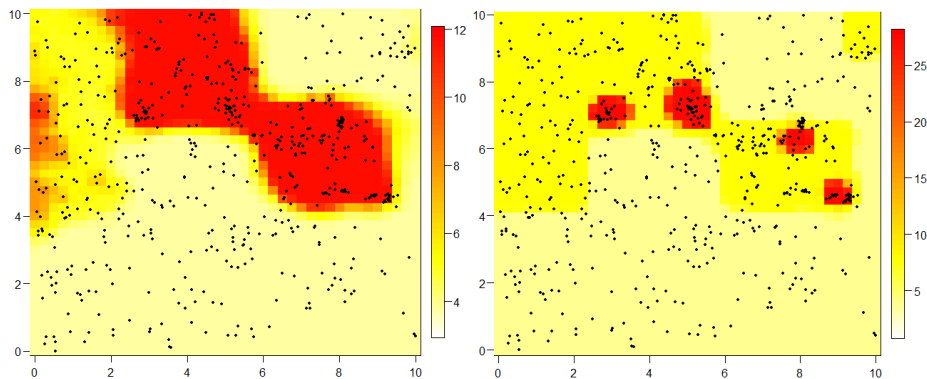


Figure 7: Posterior mean of the IF for the pinus palustris example obtained with different initial values for the MCMC chain.

The third example considers the location of 678 particles observed in a longitudinal plane section of 18×7 mm through a gradient sinter filter made from bronze powder. The original area is rescaled to $(0, 10) \times (0, 4)$ and an empirical analysis via Kernel smoothing suggests $K = 5$. The estimated IF is shown in Figure 8, which also brings the extra information about the radius of each particle. Although this information is not used in the analysis, the clear relation between radius and particle concentration was captured by the IF estimate.

Finally, the fourth example illustrates the scalability of the proposed algorithm to large datasets by considering the location of fires in a rectangular region (rotated 90° to the left and rescaled to 10.9×9.1) containing most of the area of New Brunswick, Canada, from 1987 to 2003 (excluding 1988). The estimated IF is presented in Figure 8.

5.2 Spatiotemporal example

We consider the New Brunswick fires dataset for the years 2000 to 2003. The number of fires per year is 140, 194, 127 and 94, respectively. We fit the model in (24)-(29) with three levels and perform prediction of the IF and its integral for year 2004. Results are shown in Figures 9 and 10.

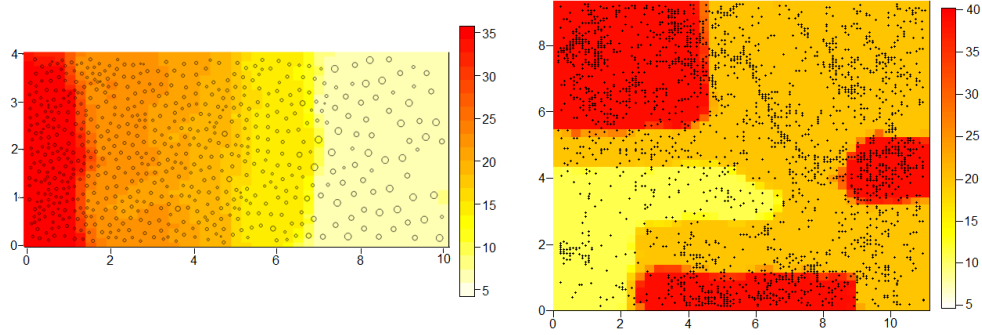


Figure 8: Posterior mean of the IF for the bronze filter example (left) and for the New Brunswick fires example (right).

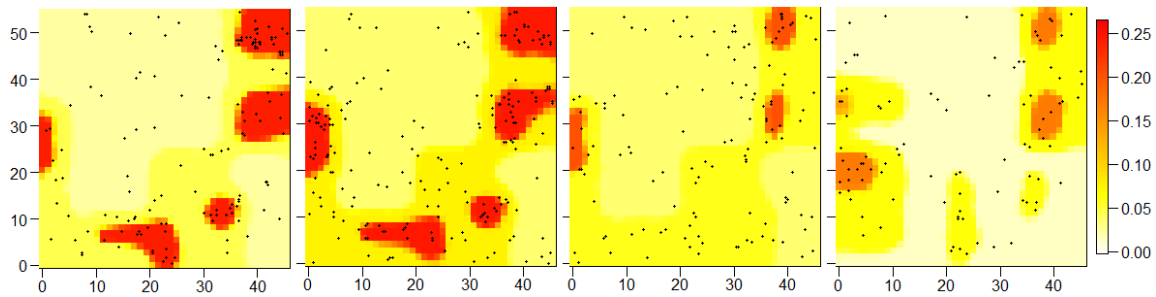


Figure 9: Posterior mean of the IF for the New Brunswick fires spatiotemporal example. Time line is left to right.

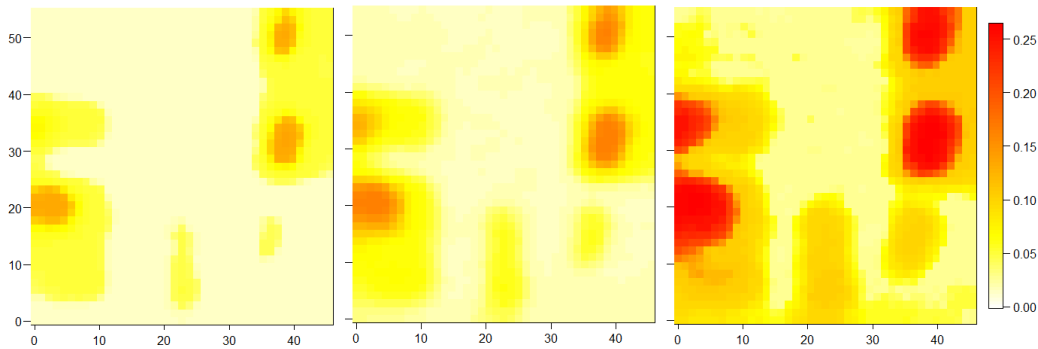


Figure 10: Predictive mean (middle) and pointwise 95% credibility interval (left and right) of the IF in year 2004 for the New Brunswick fires spatiotemporal example. The predictive mean and standard deviation of the integrated IF are 94.72 and 17.13, respectively.

6 Conclusions

This paper proposed a novel methodology to model point process phenomena using Poisson processes with piecewise constant intensity functions. The model is flexible enough to accommodate any smooth partition structure and aims at providing a more parsimonious alternative to continuous varying IF Cox process models.

An infinite-dimensional MCMC algorithm is proposed to perform exact Bayesian infer-

ence. The MCMC chain has the exact posterior distribution of all the unknown components of the model as its invariant distribution. This means the only Monte Carlo error is involved despite the intractability of the likelihood function and infinity dimensionality of the parameter space. Retrospective sampling and pseudo-marginal Metropolis are used to circumvent the infinite dimensionality and intractable likelihood problems, respectively. Efficient proposal distributions are carefully devised for the latent Gaussian process component and the pseudo-marginal auxiliary variable. Computational cost issues are mitigated by adopting a truncated covariance function for the Gaussian process prior and by adding a virtual retrospective sampling step in the MCMC algorithm that deletes extra sampled locations of the GP component.

A variety of issues related to the efficiency of the proposed MCMC algorithm are discussed and empirically explored through simulations. Model fitting regarding the choice of the number of levels for the IF is also explored. Results show a considerably good performance of the proposed methodology. A spatiotemporal extension of the level-set Cox process model is also proposed and applied to a real dataset.

The methodology proposed in this paper is the first exact (with no discretisation) approach to deal with flexible and piecewise constant IF Cox process models. We believe that this work offers a significant contribution to the field of exact methodologies for infinite-dimensional statistical problems and can contribute to further developments in this area.

Acknowledgements

The first author would like to thank FAPEMIG and CNPq for financial support. The second author would like to thank CAPES for financial support. The authors would like to thank Gareth Roberts for insightful discussions about the MCMC algorithm.

References

- Andrieu, C. and G. O. Roberts (2009). The pseudo-marginal approach for efficient monte carlo computations. *The Annals of Statistics*, 697–725.
- Andrieu, C. and M. Vihola (2015). Convergence properties of pseudo-marginal Markov chain Monte Carlo algorithms. *The Annals of Applied Probability* 25, 1030–1077.
- Baddeley, A., E. Rubak, and R. Turner (2015). *Spatial point patterns: methodology and applications with R*. Chapman and Hall/CRC.
- Beskos, A., O. Papaspiliopoulos, G. O. Roberts, and P. Fearnhead (2006). Exact and computationally efficient likelihood-based inference for discretely observed diffusion processes (with discussion). *Journal of the Royal Statistical Society. Series B* 68(3), 333–382.
- Beskos, A. and G. O. Roberts (2005). Exact simulation of diffusions. *The Annals of Applied Probability* 15(4), 2422–2444.
- Datta, A., S. Banerjee, A. O. Finley, and A. E. Gelfand (2016). Hierarchical nearest-neighbor Gaussian process models for large geostatistical datasets. *Journal of the American Statistical Association* 111, 800–812.

- Doornik, J. A. (2009). An object-oriented matrix programming language ox 6.
- Dunlop, M. M., M. A. Iglesias, and A. M. Stuart (2016). Hierarchical bayesian level set inversion. *Statistics and Computing*, 1–30.
- Frade, D. D. R. (2014). *Relações entre fatores ambientais e espécies florestais por metodologias de processos pontuais*. Ph. D. thesis, Universidade de São Paulo.
- Gamerman, D. (2010). *Handbook of Spatial Statistics*, Chapter Dynamic spatial models including spatial time series, pp. 437–448. London: CRC / Chapman & Hall.
- Gonçalves, F. B. and D. Gamerman (2018). Exact Bayesian inference in spatio-temporal Cox processes driven by multivariate Gaussian processes. *Journal of the Royal Statistical Society, Series B* 80, 157–175.
- Gonçalves, F. B., G. O. Roberts, and K. G. Łatuszynski (2017). Exact Monte Carlo likelihood-based inference for jump-diffusion processes. [*arXiv:1707.00332*].
- Gonçalves, F. B. and P. Franklin (2019). On the definition of likelihood function. [*arXiv:1906.10733*].
- Hildeman, A., D. Bolin, J. Wallin, and J. B. Illian (2018). Level set cox processes. *Spatial Statistics* 28, 169–193.
- Kingman, J. F. C. (1993). *Poisson processes*. Wiley Online Library.
- Møller, J., A. R. Syversveen, and R. P. Waagepetersen (1998). Log gaussian cox processes. *Scandinavian journal of statistics* 25(3), 451–482.
- Rao, V. and Y. W. Teh (2013). Fast MCMC sampling for Markov jump processes and extensions. *The Journal of Machine Learning Research* 14(1), 3295–3320.
- Roberts, G. O., A. Gelman, W. R. G., et al. (1997). Weak convergence and optimal scaling of random walk metropolis algorithms. *The annals of applied probability* 7(1), 110–120.
- Roberts, G. O. and J. S. Rosenthal (2009). Examples of adaptive mcmc. *Journal of Computational and Graphical Statistics* 18(2), 349–367.
- Rowlingson, B., P. Diggle, and M. R. Bivand (2012). Package splancs. *gen* 14(1).
- Silva, V. L. (2012). *Associação espaço-temporal entre mortalidade por neoplasia proximidade de antenas de telefonia celular em Belo Horizonte*. Ph. D. thesis, Universidade Federal de Minas Gerais.
- Simpson, D., J. B. Illian, F. Lindgren, S. H. Sørbye, and H. Rue (2016). Going off grid: Computationally efficient inference for log-gaussian cox processes. *Biometrika* 103(1), 49–70.
- Smith, R. L. and J. E. Miller (1986). A non-Gaussian state space model and application to prediction of records. *Journal of the Royal Statistical Society, Series B* 48, 79–88.

Appendix A - Proofs

Proof of Proposition 1

Let $I_{nk} = I_k(s_n)$ be the indicator of $s_n \in S_k$, where s_n is the n -th point from N and $I = (I_1, \dots, I_{|N|})$, where $I_n = (I_{n1}, \dots, I_{nK}) \sim \text{Mult}\left(1, \frac{\mu_1}{\mu(S)}, \dots, \frac{\mu_K}{\mu(S)}\right)$. Therefore, $E(I_{nk}) = \frac{\mu_k}{\mu(S)}$ and $\mu(S)I_{nk}$ is an unbiased estimator of μ_k . Then,

$$\begin{aligned}
E_{|N|,I}[\hat{M}] &= E_{|N|,I} \left[e^{-\mu(S)\lambda_m} \prod_{k=1}^K \left(\frac{\delta\lambda_M - \lambda_k}{\delta\lambda_M - \lambda_m} \right)^{|N_k|} \right] \\
&= E_{|N|,I} \left[e^{-\mu(S)\lambda_m} \prod_{n=1}^{|N|} \left(\frac{\delta\lambda_M - \sum_{k=1}^K I_{nk}\lambda_k}{\delta\lambda_M - \lambda_m} \right) \right] \\
&= e^{-\mu(S)\lambda_m} E_{|N|} \left[\left(\frac{\mu(S)\delta\lambda_M - \sum_{k=1}^K \mu_k\lambda_k}{\mu(S)(\delta\lambda_M - \lambda_m)} \right)^{|N|} \right] \\
&= e^{-\mu(S)(\lambda_m + \delta\lambda_M - \lambda_m)} \sum_{j=0}^{\infty} \frac{\left(\mu(S)\delta\lambda_M - \sum_{k=1}^K \mu_k\lambda_k \right)^j}{j!} \\
&= e^{-\sum_{k=1}^K \mu_k\lambda_k} = M.
\end{aligned} \tag{35}$$

Proof of Proposition 2

We shall compute the variance of $\hat{M}_1 = \prod_{k=1}^K \left(\frac{\delta\lambda_M - \lambda_k}{\delta\lambda_M - \lambda_m} \right)^{|N_k|}$.

We use the basic probability result that if $X \sim \text{Poisson}(\lambda)$, then $E[a^{nX}] = \exp\{-\lambda(1-a^n)\}$, $n \in \mathbb{N}$, and the fact that $|N_k| \sim \text{Poisson}(\mu_k\lambda^*)$ to compute $E[\hat{M}_1^2]$ and $E[\hat{M}_1]$ and obtain

$$\begin{aligned}
\text{Var}(\hat{M}_1) &= \exp \left\{ -\sum_{k=1}^K \mu_k(\delta\lambda_M - \lambda_m) \left[1 - \left(\frac{\delta\lambda_M - \lambda_k}{\delta\lambda_M - \lambda_m} \right)^2 \right] \right\} \\
&\quad - \exp \left\{ -2\sum_{k=1}^K \mu_k(\lambda_k - \lambda_m) \right\},
\end{aligned}$$

implying that

$$\text{Var}(\hat{M}) = \exp\{-2\mu(S)\lambda_m\} \text{Var}(\hat{M}_1).$$

Finally,

$$\frac{\partial \text{Var}(\hat{M}_1)}{\partial \delta} = \exp(\kappa) \left[\sum_{k=1}^K \mu_k\lambda_M \left(\left(\frac{\delta\lambda_M - \lambda_k}{\delta\lambda_M - \lambda_m} \right)^2 - 2(\delta\lambda_M - \lambda_k) - 1 \right) \right] < 0,$$

onde $\kappa \in \mathbb{R}$.

Appendix B - The MCMC algorithm

Algorithm 1 MCMC for the level-set Cox process model

Input: $K, L, \delta, \tau^2, r, p_N, J_\lambda$, and initial values for N, β, λ, c .

Output: MCMC posterior sample of θ .

- 1: Choose, uniformly, a proportion p_N of the locations in N and fix the values of β at those locations.
 - 2: Proposed β at the remaining locations of N and at the locations of Y from the GP prior conditional on the values at the fixed locations.
 - 3: Accept the proposal w.p. given in (14).
 - 4: **for** $j = 1 \rightarrow L$ **do**
 - 5: For the j -th square, propose to add or remove a location according to the probabilities in (12).
 - 6: If an addition is proposed, simulate the location uniformly in the cylinder of base given by the j -th square and height λ^* and simulate β at that location from the GP prior conditional on its values at $\{Y, N\}$.
 - 7: If a removal is proposed, choose uniformly among the existing locations above the j -th square.
 - 8: Accept the proposal w.p. given in (13).
 - 9: Perform virtual update (delete all the values of β in $S \setminus \{Y, N\}$).
 - 10: **end for**
 - 11: **for** $j = 1 \rightarrow J_\lambda$ **do**
 - 12: Propose λ from a properly tuned Gaussian random walk.
 - 13: If the proposed value of λ yields a value $\check{\lambda}^*$ larger than the current one λ^* , simulate N^* between the current and proposal values of λ^* - simulate the number of locations from a $Poisson((\check{\lambda}^* - \lambda^*)\mu(S))$ and distribute them uniformly in the section of the cylinder.
 - 14: If extra locations of N^* are simulated in the previous step, simulate β at those locations from the GP prior conditional on its values at $\{Y, N\}$.
 - 15: Accept the proposed value of λ w.p. given in (15).
 - 16: Perform virtual update (delete all the values of β in $S \setminus \{Y, N\}$).
 - 17: **end for**
 - 18: If c is not fixed, propose c from a properly tuned uniform random walk and accept w.p. given in (16).
 - 19: If enough iterations of the MCMC have been performed, stop; otherwise, go back to 1.
-

The virtual update is performed if the set of unveiled location of β in $S \setminus \{Y, N\}$ is not empty. The tuning of the random walk proposal is performed in a pre-run of the algorithm.

Appendix C - Further results from the simulations

Figure 11 shows the trace plots and ACF plots of the pseudo-marginal likelihood function (middle) and of the integrated IF (bottom) for the example in Section 4.1 with $\tau^2 = 5$, $r = 1$, $\delta = 5$ and $K = 3$.

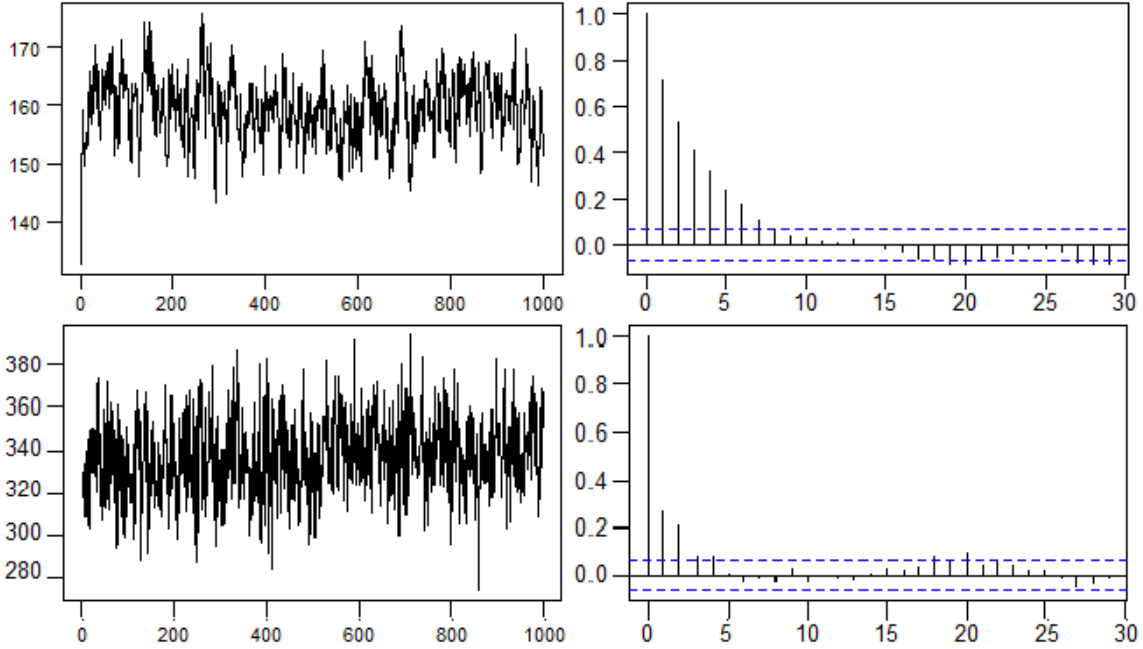


Figure 11: Trace plots and ACF plots of the pseudo-marginal likelihood function (top) and of the integrated IF (bottom).

Figure 12 shows the two initial partitions used to run the MCMC with the respective trace plots of the pseudo-marginal likelihood function. For both cases, the initial value of all the λ_k 's is $|Y|/\mu(S)$. It can be noticed how the MCMC algorithm takes considerably longer to converge when the initial partition is considerably different from the true one.

Figure 13 shows the estimated IF in each of the 9 specifications in the sensitivity analysis in Section 4.1.

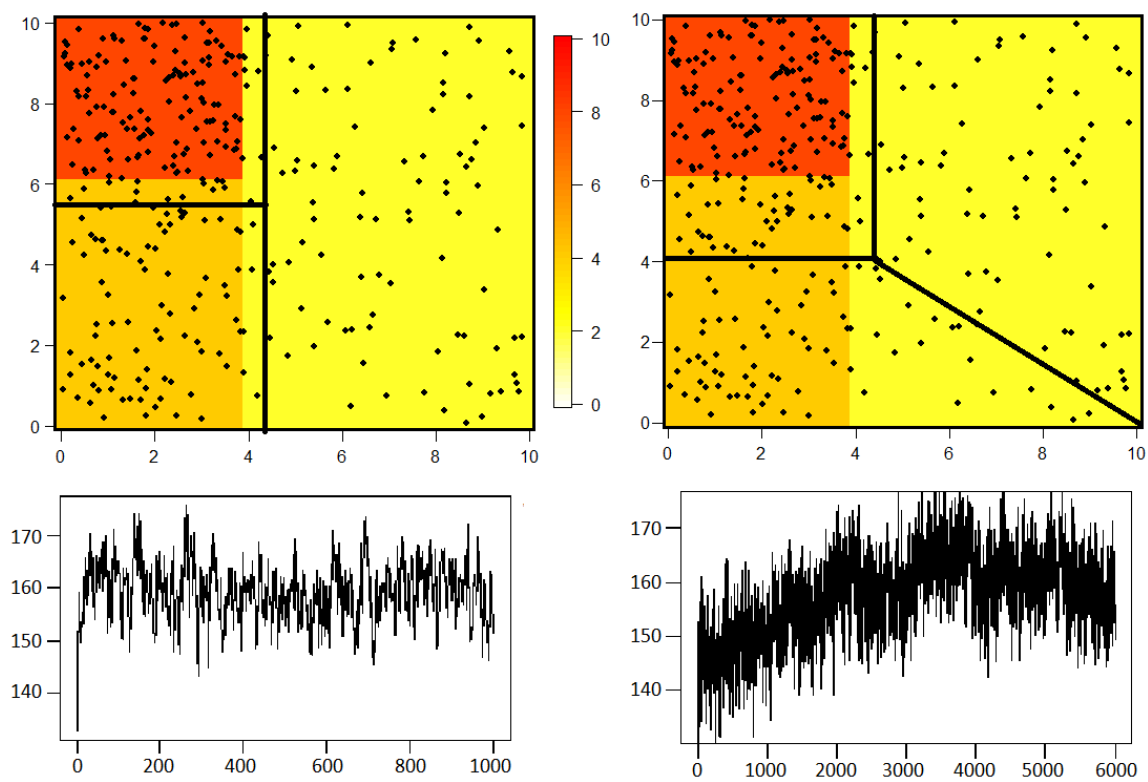


Figure 12: Initial values of the partition and the respective trace plots of the pseudo-marginal likelihood function.

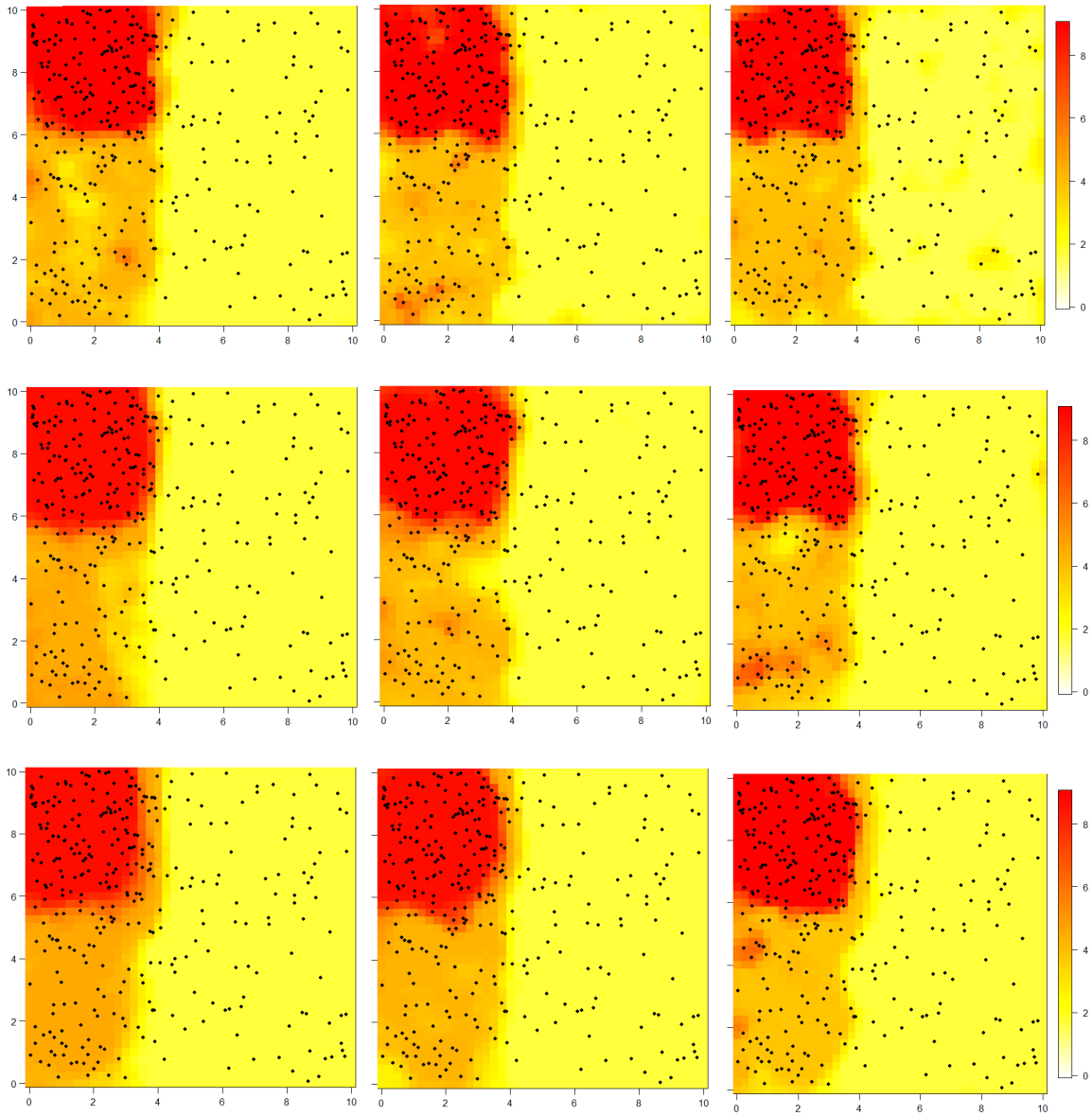


Figure 13: Posterior mean of the IF for the nine different prior specifications. Each row refers to a different τ^2 , in ascending order, and each columns refers to a different r , also in ascending order.